Biomaterials Science

ROYAL SOCIETY OF CHEMISTRY

PAPER

View Article Online
View Journal | View Issue

Cite this: *Biomater. Sci.*, 2025, **13**, 1222

Ganglioside-incorporating lipid nanoparticles as a polyethylene glycol-free mRNA delivery platform†

Yafi S. Permana,[a] Mincheol Jang,[a] Kyunghwan Yeom,[a] Erinn Fagan,[a] Yong Jae Kim,[b] Joon Hyeok Choi[b] and Ji-Ho Park *[a]

Received 13th October 2024,
Accepted 3rd January 2025

DOI: 10.1039/d4bm01360c

rsc.li/biomaterials-science

Incorporation of polyethylene glycol (PEG) is widely used in lipid nanoparticle (LNP) formulation in order to achieve adequate stability due to its stealth properties. However, studies have detected the presence of anti-PEG neutralizing antibodies after PEGylated LNP treatment, which are associated with anaphylaxis, accelerated LNP clearance and premature release of cargo. Here, we report the development of LNPs incorporating ganglioside, a naturally occurring stealth lipid, as a PEG-free alternative. Physicochemical characterization showed that ganglioside-LNPs exhibited superior stability throughout prolonged cold storage compared to stealth-free LNPs, preventing particle aggregation. Additionally, there was no significant change in particle size after serum incubation, indicating the ability of ganglioside to prevent unwanted serum protein adsorption. These results exemplify the effective stealth properties of ganglioside. Furthermore, ganglioside-LNPs exhibited significantly higher mRNA transfection *in vivo* after intravenous administration compared to stealth-free LNPs. The ability of ganglioside to confer excellent stealth properties to LNPs while still enabling *in vivo* mRNA expression makes it a promising candidate as a natural substitute for immunogenic PEG in mRNA-LNP delivery platforms, contributing to the future advancement of gene therapy.

1. Introduction

mRNA-based therapy has become an impressive tool in clinical applications, providing a blueprint for functional protein production inside the human body. However, due to the presence of physiological barriers that inhibit the functionality of mRNA,[1–5] a delivery vehicle that can protect mRNA and enhance its uptake is needed. Lipid nanoparticles (LNPs) have been reported to encapsulate mRNA, thereby protecting it from degradation.[1,6] The standard components of LNPs include ionizable cationic lipids, helper phospholipids, cholesterol, and polyethylene glycol (PEG)-anchored lipids.[7,8] LNPs have emerged as cutting-edge technology for delivering mRNA vaccines in response to the COVID-19 pandemic.[9–11] Additionally, LNP research has been expanded to a broad range of protein replacement therapy applications, such as vascular endothelial growth factor A (VEGFA), interleukin 12 (IL-12), and p53.[12–14] Furthermore, LNPs have been shown to mediate the delivery of CRISPR-Cas9 mRNA, enabling the treatment of various genetic disorders.[15,16]

PEG-anchored lipids play a vital role in conferring stealth properties to LNPs. The hydrophilic PEG forms a steric barrier surrounding each particle, which repels neighboring particles, thereby preventing aggregation.[17] Additionally, the barrier also works against serum proteins, thus reducing particle clearance and prolonging circulation time.[18–20] It is rarely discussed that our cell membranes are also equipped with natural stabilizing molecules, *i.e.* glycolipids. One of the most abundant glycolipids is ganglioside, which is predominantly found in the brain, where it plays a pivotal role in cell–cell recognition and in initiating cell communication.[21–23] Ganglioside is an amphiphilic molecule containing a hydrophobic ceramide tail and a hydrophilic glycan headgroup connected through a glycosidic linkage.[22] Its hydrophobic property allows it to participate in van der Waals interactions with other lipids, stabilizing ganglioside within lipid membranes.[22] Its hydrophilic chain extends outward, exposing the sialic acid moiety that underlies the role of ganglioside in cell communication.[22] The outward localization of the hydrophilic group also creates a hydrophilic steric barrier, suggesting the potential of ganglioside to confer stealth properties.[24] The utilization of ganglioside to confer stealth characteristics to nanoparticles has been explored. Studies on the pharmacokinetics of liposomes demonstrated prolonged biodistribution with ganglioside incorporation in a

[a]*Department of Bio and Brain Engineering, and KAIST Institute for Health Science and Technology, Korea Advanced Institute of Science and Technology (KAIST), Daejeon 34141, Republic of Korea. E-mail: jihopark@kaist.ac.kr*
[b]*R&D, De novo Biotherapeutics, S-tower 17F, Saemunan-ro 82, Jongno-gu, Seoul, 03185, Republic of Korea*

† Electronic supplementary information (ESI) available. See DOI: https://doi.org/10.1039/d4bm01360c

comparable manner to PEGylated liposomes.[25,26] On top of that, ganglioside incorporation was reported to lower the adsorption of serum proteins, particularly complement C3 protein, supporting the role of ganglioside in decreasing complement activation.[27] Additionally, incubation of calcein-loaded liposomes with human plasma demonstrated a reduction of free calcein after ganglioside incorporation, which implies that gangliosides inhibit the premature release of cargo.[25] Altogether, ganglioside incorporation in nanoparticles has immense potential to provide stealth properties.

In this study, we develop ganglioside-incorporating LNPs (ganglioside-LNPs) as a PEG-free mRNA delivery system. Optimization of the LNP formulation process and composition is conducted based on the analysis of physicochemical properties and *in vitro* transfection efficiency. Size characterization of the optimized ganglioside-LNPs upon cold storage shows that ganglioside incorporation prevented particle aggregation, demonstrating comparable stability to conventional PEG-LNPs. In order to simulate *in vivo* stability, we also assess changes in particle size after incubation in serum, showing that ganglioside incorporation inhibits serum protein adsorption. Finally, we evaluate the *in vivo* transfection efficiency of ganglioside-LNPs after intravenous administration, reporting a greater than 3-fold increase compared to stealth-free LNPs. Collectively, the incorporation of ganglioside as an alternative for PEG in mRNA-LNPs is a promising approach to maintain particle stability and stealth properties while still facilitating mRNA transfection.

2. Experimental section

2.1. Materials

Firefly luciferase (fLuc) pDNA was obtained from De Novo Biotherapeutics (Seoul, Republic of Korea). Ionizable lipid (6*Z*,9*Z*,28*Z*,31*Z*)-heptatriaconta-6,9,28,31-tetraen-19-yl 4-(dimethylamino)butanoate (DLin-MC3-DMA, MC3) was purchased from MedChemExpress (Princeton, NJ). 1,2-Distearoyl-*sn-glycero*-3-phosphocholine (DSPC), cholesterol, ganglioside-total (porcine brain), and 1,2-dimyristoyl-*rac-glycero*-3-methoxypolyethylene glycol-2000 (DMG-PEG_{2k}) were all purchased from Avanti Polar Lipids (Alabaster, AL). Deionized water was obtained using a Millipore Milli-Q system (Merck Millipore, Darmstadt, Germany). Ethyl alcohol (HPLC/spectrophotometric grade), D-(+)-glucose (≥99.5%), 1× phosphate-buffered saline (PBS), sodium citrate tribasic dihydrate (ACS reagent, ≥99.0%), and citric acid (ACS reagent, ≥99.5%) were purchased from Sigma-Aldrich (Poole, UK).

2.2. *In vitro* transcription of fLuc mRNA

Prior to transcription, fLuc pDNA was linearized using BbsI-HF in rCutSmart buffer (New England Biolabs, MA). After a 2-hour incubation, the linearized pDNA was purified using the QIAquick PCR purification kit (Qiagen, NC). Firefly luciferase mRNA was synthesized using the HiScribe™ T7 mRNA kit with CleanCap® Reagent AG (New England Biolabs). In order to decrease the immunogenicity of the mRNA, we used *N*1-methyl-pseudo-UTP (Jena Bioscience, Jena, UK) as a substitute for UTP. After a 3-hour incubation at 37 °C, mRNA was purified using the Monarch® RNA Cleanup Kit (New England Biolabs). All purified mRNA was then stored at −80 °C.

2.3. Preparation of LNPs

An organic phase was first prepared by mixing the lipids, MC3, DSPC, cholesterol, and ganglioside. The solvent was then evaporated through two hours of desiccation to generate a lipid film. The film was then rehydrated with ethanol to a lipid concentration of 1 mg mL^{-1} and sonicated for 30 seconds. An aqueous phase was prepared by diluting mRNA in 50 mM citrate buffer. The aqueous phase and organic phase were then rapidly mixed *via* pipetting at a volume ratio (A/O) of 3 : 1. The mixture was then incubated for 10 minutes at room temperature (RT) to allow for the self-assembly of all components into LNPs. In order to remove the ethanol, the mixture was then dialyzed using SnakeSkin™ dialysis tubing (10 kDa molecular weight cutoff, 16 mm; Thermo Fisher Scientific, Loughborough, UK) for six hours. The dialysis was performed at 4 °C with stirring. LNP preparation also included the formulation of stealth-free LNPs and PEG-LNPs. Stealth-free LNPs were composed of MC3, DSPC, and cholesterol at a molar ratio of 50 : 10 : 40. PEG-LNPs were composed of MC3, DSPC, cholesterol, and DMG-PEG_{2k} at a molar ratio of 50 : 10 : 38.5 : 1.5.[28]

2.4. Characterization of LNPs

After dialysis, the hydrodynamic diameter and polydispersity index (PDI) of LNPs were measured using Malvern Nano Zetasizer (Malvern Instruments Ltd, Malvern, U.K.). This instrument was also used to measure the zeta-potential of LNPs at physiological pH. Prior to zeta-potential measurement, 20 μL of the samples were diluted in 800 μL of 0.1× PBS (pH 7.4). Encapsulation efficiency was determined using the Quant-iT™ RiboGreen™ RNA assay kit (Thermo Fisher Scientific). LNPs were diluted to approximately 650 ng mL^{-1} of mRNA in 1× TE buffer. The dilution was also performed in the presence of 0.5% Triton X-100 (Sigma Aldrich), which disrupts lipid membranes, making all mRNA unencapsulated. 100 μL of each solution was then pipetted into a 96-well black plate. Afterwards, 100 μL of 1× RiboGreen™ reagent, which quantifies unencapsulated mRNA, was pipetted into each well, followed by the measurement of fluorescence intensity (SpectraMax Gemini™, Molecular Devices) at excitation and emission wavelengths of 485 nm and 525 nm, respectively. Calibration curves of fluorescence intensity *versus* mRNA concentration in TE buffer and Triton X-100 solution were recorded using a serial dilution of mRNA concentrations. The encapsulation efficiency (EE) of the samples was calculated as follows:

$$EE = \frac{C_{TX} - C_{TE}}{C_{TX}} \quad (1)$$

where C_{TX} and C_{TE} are the RNA concentrations in Triton X-100 and TE buffer, respectively.

2.5. Characterization of LNPs upon cold storage and incubation in serum

The diameter of optimized ganglioside-LNPs upon cold storage was measured in order to evaluate the stability of LNPs conferred by ganglioside. Samples were stored at 4 °C, and diameter measurements were conducted on days 2, 3, 5, 7, and 14. An increase in diameter indicates the aggregation of particles. Stealth-free LNPs and PEG-LNPs were also evaluated as controls. In addition, the measurement of particle size upon incubation in serum was performed to demonstrate the stability of particles during *in vivo* circulation. The serum solution was prepared by diluting fetal bovine serum (FBS, HyClone™, Logan, UT) to a concentration of 10% in pH 7.4 PBS. Ganglioside-LNPs were added to the serum solution at a volume ratio of 1 : 5, which demonstrates the dilution of sample upon treatment. Immediately following dilution, the diameter of particles was assessed. The LNPs in serum were then stored at 37 °C. Particle diameter was measured again at 2, 4, 6, and 24 hours after particle dilution. Stealth-free LNPs and PEG-LNPs were also evaluated as controls.

2.6. Cell culture and *in vitro* luciferase expression

Human embryonic kidney 293T (HEK293T, ATCC) cells were grown in Dulbecco's modified Eagle's medium (HyClone™) supplemented with 10% FBS (HyClone™) and 2× penicillin–streptomycin (HyClone™) at 37 °C in a 5% CO_2 environment. The cells were passaged using Gibco™ trypsin–EDTA (Thermo Fisher Scientific). For transfection experiments, the cells were seeded at 14 000 cells per well in a black flat-bottom 96-well plate and allowed to grow for 24 h prior to transfection. Ganglioside-LNPs were added to the cells at a final mRNA dose of 60 ng per well. After 48 h, the medium was removed to leave a final volume of 50 μL and reconstituted Bio-Glo™ luciferase assay substrate (Madison, WI) was added at a 1 : 1 volume ratio to each well. Following 5 minutes of RT incubation, luminescence from each well was recorded using an IVIS Lumina system (PerkinElmer, Waltham, MA). Stealth-free LNPs and PEG-LNPs were also treated as controls. Results were quantified as total flux (photons per s) and shown as mean ± standard deviation of three replicates.

2.7. Animals

All animal procedures were performed in accordance with the Guidelines for Care and Use of Laboratory Animals of Korea Advanced Institute of Science and Technology (KAIST) and approved by the Institutional Animal Care and Use Committee (IACUC) (approval no. KA2021-117). Healthy, 7-week-old female C57BL/6 mice (N = 3) were obtained from KOATECH (Gyeonggi-do, Republic of Korea). All mice were acclimated to the animal facility for 1 week prior to use in experiments.

2.8. *In vivo* luciferase mRNA delivery

Following sedation by intramuscular injection of Zoletil™, ganglioside-LNPs at a concentration of 40 μg mL^{-1} were administered intravenously to mice *via* retroorbital injection at a dose of 4 μg fLuc mRNA. After 24 h, 100 μL of reconstituted luciferase assay substrate (In Vivo-Glo™) was administered intraperitoneally. Bioluminescence from the whole body and harvested organs (lungs, heart, spleen, kidneys, and liver) was imaged within 10–25 minutes following substrate administration using the IVIS Lumina system (PerkinElmer). Stealth-free LNPs and PEG-LNPs were also injected as controls. The luminescence results were calibrated as total flux (photons per s) and shown as mean ± standard deviation.

2.9. Data analysis

All statistical analysis was conducted using GraphPad Prism 8 software. Error bars represent one standard deviation. To compare two groups, an unpaired t-test was performed, assuming Gaussian distribution. Groups of three or more were compared by one-way ANOVA. To compare responses generated at different time points, two-way ANOVA was performed. Statistical significance is indicated by $*p \leq 0.05$, $**p \leq 0.01$, and $***p \leq 0.0001$.

3. Results and discussion

3.1. Adaptation of the standard LNP formulation procedure for ganglioside-LNPs

Incorporation of ganglioside into LNP formulations using the standard protocol resulted in particle aggregation at multiple steps. Therefore, we first sought to optimize the parameters of LNP formulation for ganglioside-LNP preparation. According to DLVO theory, which demonstrates the stabilization of a colloidal system, there are several approaches for improving particle stability (ESI†), including increasing the surface potential of the particles and decreasing the ion concentration of the solvent.[29] Citrate buffer with pH 4 is commonly used for the aqueous phase to dilute the mRNA prior to mixing with the lipids. Reducing the buffer pH to 3 generates more stable ganglioside-LNPs due to the increased particle surface potential, resulting in stronger repulsive interactions with adjacent particles (Fig. 1a). After formulation, LNPs are typically dialyzed in 1× PBS. Using deionized water as the dialyzing fluid prevents the aggregation of ganglioside-LNPs, owing to the absence of any ions and the consequent decrease in charge shielding (Fig. 1b). However, prior to administration into biological systems, additional dilution in an isotonic solution should be performed. Dilution of ganglioside-LNPs in the standard solvent 1× PBS remarkably enlarged the particles, although the diameter still met the criteria of sterile-filtration (less than 215 nm) (Fig. 1c). In contrast, dilution of ganglioside-LNPs in 5% dextrose in water (D5W) avoids considerable particle swelling due to the absence of electrolytes (Fig. 1c). Moreover, an *in vitro* luciferase assay using HEK293T cells showed that D5W-diluted ganglioside-LNP treatment exhibited a 1.75-fold improvement in transfection efficiency compared to particles diluted in PBS (Fig. 1d). Taken together, substitution of pH 3 citrate buffer, deionized water, and D5W for the aqueous phase solution, dialyzing fluid, and intravenous fluid,

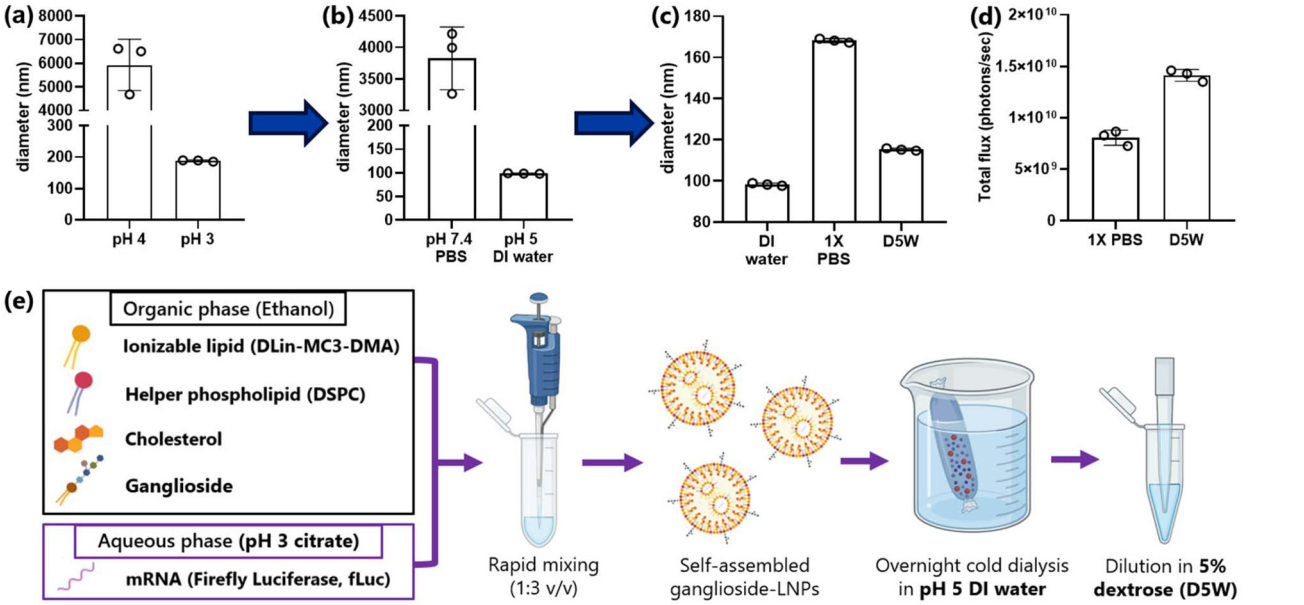

Fig. 1 Adjustment of LNP formulation parameters for ganglioside-LNP preparation. (a) Effect of the pH of citrate buffer on the diameter of ganglioside-LNPs after mixing the lipids and mRNA. (b) Effect of dialyzing fluid on the diameter of ganglioside-LNPs after dialysis. (c and d) Effect of final isotonic solvent on the diameter (c) and the transfection efficiency (d) of ganglioside-LNPs (N = 3). (e) Scheme of the ganglioside-LNP preparation protocol. Lipids were mixed, desiccated to generate a lipid film and then dissolved in pure ethanol. In parallel, mRNA was diluted in a 50 mM citrate buffer with a pH of 3. LNP formulation was performed by rapid mixing of the two phases, followed by RT incubation for 10 minutes to allow for self-assembly of all the components. Particles were then dialyzed in deionized (DI) water at 8 °C with constant stirring in order to remove the ethanol. Finally, LNPs were diluted in 5% dextrose (D5W) to generate an injectable solution with the same osmolarity as blood.

respectively, was adopted for future formulations of ganglioside-LNPs. The preparation of ganglioside-LNPs is illustrated in Fig. 1e.

3.2. *In vitro* optimization of ganglioside-LNP composition

Ganglioside-LNPs were optimized *in vitro* to identify the composition with superior characteristics. In addition to enabling the greatest transfection efficiency, all formulations should meet several criteria for physicochemical properties: (1) the diameter of particles should be less than 215 nm in order to allow sterile filtration,[30] (2) the polydispersity index (PDI) should not exceed 0.2 to indicate monodisperse nanoparticles,[31] and (3) the encapsulation efficiency should be at least 80% to enable sufficient mRNA delivery.[32]

For the first phase of optimization, the ganglioside content was varied by attempting several mole percentages. While fixing the lipid molar ratios of MC3 and DSPC to 50% and 10%, respectively, the remaining 40% was divided between cholesterol and ganglioside. The incorporation of 50% MC3 was found to confer suitable mRNA encapsulation as well as the greatest transfection efficiency in ganglioside-LNPs (ESI Fig. 1†). A broad range of ganglioside concentrations were first assessed, covering 0.016–1.5 mol%. There was an inverse correlation between ganglioside incorporation and the resulting particle zeta-potential (ESI Fig. 2a†). While all formulations met the criteria for diameter (<215 nm) and PDI (≤0.2) (ESI Fig. 2b and c†), the encapsulation efficiency fell under the threshold (80%) after ganglioside incorporation was reduced below 0.125% (ESI Fig. 2d†). For the second phase, the groups were expanded over a narrower range of ganglioside concentrations, covering 0.25–1.5%, and evaluated to determine the optimal concentration of ganglioside. Consistent with the previous measurements (ESI Fig. 2d†), all formulations with 0.25–1.5% ganglioside meet the criteria for diameter (<215 nm), PDI (≤0.2), and encapsulation efficiency (≥80%) (Fig. 2a–c). Treatment of LNPs *in vitro* revealed that LNPs with 0.25% ganglioside exhibited the highest transfection efficiency, which gradually decreased with increasing concentrations of ganglioside (Fig. 2d). It is important to note that while stealth-lipid incorporation is necessary to prevent particle agglomeration and serum protein adsorption, high concentrations of stealth-lipid hinder cellular internalization.[17] This is because, at higher surface densities, the polymer chains become more tightly packed and adopt a straight, brush-like arrangement, forming a stronger hydrophilic barrier that reduces interaction with the cellular membrane. The previous study also demonstrated that increasing PEG-lipid concentrations beyond 1.5% gradually reduced mRNA transfection efficiency *in vitro*.[33] Therefore, an intermediate molar ratio of ganglioside, particularly 0.25% incorporation, mediates optimal transfection efficiencies. Taken together, the two-phase screening identified 0.25% as the optimal ganglioside concentration, which was adopted for all future formulations.

Afterwards, the molar ratio between the ionizable lipid amine groups and the nucleotide phosphate groups (N/P ratio)

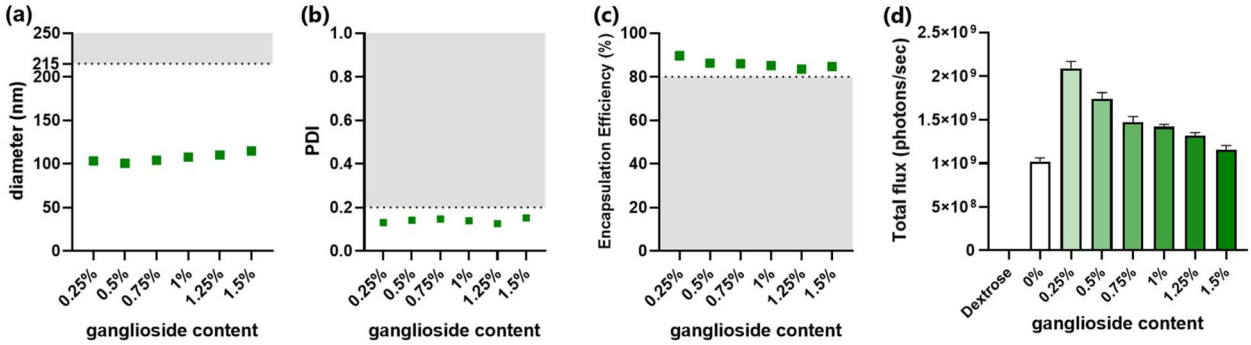

Fig. 2 Characterization of ganglioside-LNP formulations with varying mol percentages of ganglioside. (a) Particle size was measured using dynamic light scattering (DLS). The horizontal line at 215 nm indicates the cutoff for sterile filtration. (b) PDI was measured using DLS. The horizontal line at 0.2 indicates the cutoff for polydispersity. (c) mRNA encapsulation efficiencies (EE) of candidate LNPs. The horizontal line at 80% EE indicates the cutoff for insufficient mRNA encapsulation. (d) *In vitro* transfection efficiency of candidate LNPs in HEK293T cells. Bioluminescence data were quantified as total flux (photons per s) (N = 3). As a control, cells were treated with the 5% dextrose (D5W) solution.

was optimized. The molar percentages of all components were fixed at 50%, 10%, 39.75%, and 0.25% for MC3, DSPC, cholesterol, and ganglioside, respectively. All formulations met the criteria for PDI (≤0.2), indicating a narrow distribution of particle size (Fig. 3b). However, particles formulated with an N/P ratio of 1 : 1 had sizes exceeding the threshold (215 nm) (Fig. 3a). This could be attributed to increased interactions of lipids with nucleotides at lower N/P ratios, resulting in a greater number of mRNA copies encapsulated per particle. In addition to increased size, the formulation with an N/P ratio of 1 : 1 failed to encapsulate acceptable amounts of mRNA (Fig. 3c). In line with the poor encapsulation efficiency, LNPs with an N/P ratio of 1 : 1 exhibited a relatively low transfection efficiency (Fig. 3d). Considering the requirement for a sufficient amount of lipids to properly encapsulate mRNA, increasing the N/P ratio to 3 : 1 dramatically lowered the size of ganglioside-LNPs, enhanced the encapsulation efficiency, and exhibited the highest transfection efficiency (Fig. 3a–d). The diameter continuously declined with the increase in the N/P ratio, indicating a smaller amount of encapsulated mRNA per particle (Fig. 3a). Interestingly, a downward trend was also observed in the transfection efficiency of formulations with an N/P ratio higher than 3 (Fig. 3d). A possible explanation could be that increasing the N/P ratio generates a greater number of particles but with a lower density of mRNA, resulting in a competition between the particles to be endocytosed, reducing the total amount of internalized mRNA. Taken together, the LNPs with an N/P ratio of 3 : 1 demonstrated both satisfactory size and mRNA encapsulation, as well as optimal transfection efficiency, leading to its selection as the optimized N/P ratio for ganglioside-LNP formulation.

The optimized composition of ganglioside-LNPs consists of MC3, DSPC, cholesterol, and ganglioside with molar ratios of 50%, 10%, 39.75%, and 0.25%, respectively, and an N/P ratio of 3 : 1. The ganglioside-LNPs were compared to two controls: PEGylated LNPs as a positive control and stealth-free LNPs, which do not contain PEG-lipid nor ganglioside. All formulations exhibited similar physicochemical properties, includ-

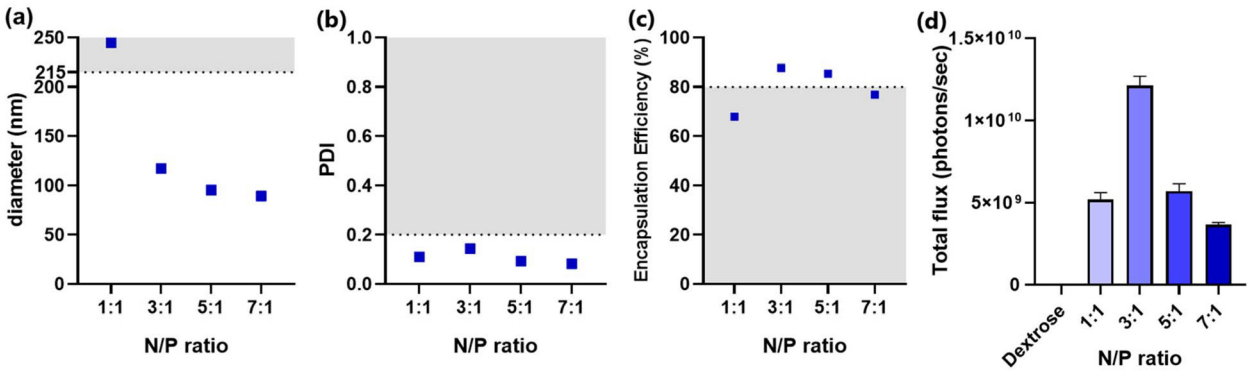

Fig. 3 Characterization of ganglioside-LNP formulations with varying N/P ratios. (a) Particle size was measured using dynamic light scattering (DLS). The horizontal line at 215 nm indicates the cutoff for sterile filtration. (b) PDI was measured using DLS. The horizontal line at 0.2 indicates the cutoff for polydispersity. (c) mRNA encapsulation efficiencies (EE) of candidate LNPs. The horizontal line at 80% EE indicates the cutoff for insufficient mRNA encapsulation. (d) *In vitro* transfection efficiency of candidate LNPs in HEK293T cells. Bioluminescence data were quantified as total flux (photons per s) (N = 3). As a control, cells were treated with the 5% dextrose (D5W) solution.

ing a narrow size distribution ranging from 100 to 110 nm, a slightly negative zeta-potential, and acceptable mRNA encapsulation efficiency (Table 1). This uniformity between LNP compositions reduces the confounding influence of physicochemical properties that could potentially affect the transfection efficiency.

Ganglioside incorporation enhanced the *in vitro* transfection efficiency of stealth-free LNPs (Fig. 4). More importantly, the treatment of optimized ganglioside-LNPs exhibits a 1.3-fold improvement in *in vitro* mRNA transfection efficiency in comparison with PEG-LNPs (Fig. 4). This finding is in line with the finding that longer hydrophilic chains inhibit the uptake by the targeted cells as well as interaction with the endosomal membrane.[34] PEG chains have longer hydrophilic chains, making them more likely to hinder the cellular uptake of the LNPs. Additionally, these longer hydrophilic chains can reduce the ability of the nanoparticle to disrupt or penetrate the endosomal membrane due to their repelling, water-attracting properties. Meanwhile, ganglioside, which has a shorter hydrophilic chain, is suggested to have a closer interaction with the cell and endosomal membrane, thereby enhancing the therapeutic efficacy of the delivery system.

Table 1 Diameter, polydispersity index (PDI), zeta-potential, and encapsulation efficiency (EE) of PEG-LNPs, stealth-free LNPs, and optimized ganglioside-LNPs

Parameter	PEG-LNP	Stealth-free LNP	Ganglioside-LNP
Diameter (nm)	103.03	106.70	106.10
PDI	0.090	0.136	0.126
Zeta-potential (mV); in pH 7.4	−1.48	−3.35	−2.90
EE (%)	94.67	83.33	84.57

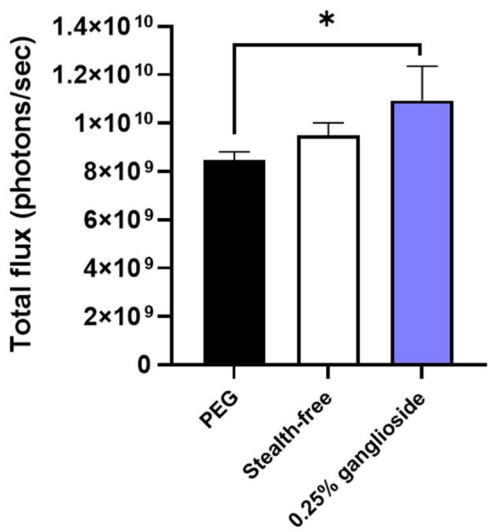

Fig. 4 *In vitro* transfection efficiency of optimized ganglioside-LNPs. Transfection efficiency was assessed in HEK293T cells. Bioluminescence data were quantified as total flux (photons per s) (N = 3). PEG-LNPs and stealth-free LNPs were treated as controls (N = 3). Significance was determined using one-way ANOVA. Note: *: $p \leq 0.05$.

3.3. Particle characterization upon prolonged cold storage and incubation in serum

In order to demonstrate the stealth properties conferred by ganglioside, particle size measurements were performed upon prolonged cold storage and incubation in serum. The formation of a steric barrier by stealth-lipids allows each particle to repel adjacent particles, thus preventing particle aggregation and enhancing the stability over time. Additionally, the external barrier prevents the adsorption of serum proteins, leading to reduced particle clearance and extended biodistribution.[19,20]

Due to the tendency of biochemical agents to undergo accelerated degradation at higher temperatures, all biopharmaceuticals, particularly those containing mRNA, should be stored at low temperatures.[34] Additionally, in order to maintain the morphology of LNPs, storage under conditions below the phase transition temperature is required. Therefore, storage in a cold environment (4 °C) was chosen for the characterization of particles over time. Size measurements were conducted periodically over the span of two weeks. Results showed that while stealth-free LNPs exhibited a notable size increase (18.5 ± 1.0 nm), ganglioside incorporation was able to significantly attenuate this enlargement, with only a slight increase (6.6 ± 0.4 nm) (Fig. 5a and b). Moreover, no difference in diameter changes between PEG-LNPs and ganglioside-LNPs was observed (Fig. 5b).

Due to the abundance of serum proteins in the blood, particle characterization following serum incubation can help predict their fate during *in vivo* systemic circulation. This study utilized 10% fetal bovine serum (FBS) as a model to evaluate particle stability in a serum environment. Size measurements showed that FBS has an average diameter of 14 nm, which remained unchanged over 24 hours, implying that serum proteins do not interfere with the measurement of particle diameter (ESI Fig. 3†). Interestingly, the exposure of PEG-LNPs to FBS resulted in a decrease in diameter over time (Fig. 5c). These results may reflect the occurrence of PEG shedding, in which PEG lipids are removed from the particle surface by exchanging with serum proteins. This is consistent with previous reports stating that PEG shedding is an important mechanism for diminishing steric shielding and consequently facilitating enhanced cellular uptake and endosomal escape.[35,36] Additionally, our data showed that the particle size decreased within 2 hours, which aligns with another study that demonstrated PEG desorption within 30 minutes.[37] On the other hand, stealth-free LNPs exhibited a significant increase in diameter following incubation in serum, suggesting the adsorption of serum proteins on the surface (Fig. 5c). Due to the absence of clearance mechanisms such as phagocytosis in the *in vitro* setting, the binding of serum proteins would not significantly affect the transfection efficiency of stealth-free LNPs. However, due to the reticuloendothelial system in the *in vivo* environment, association with serum proteins is likely to result in the rapid elimination of stealth-free

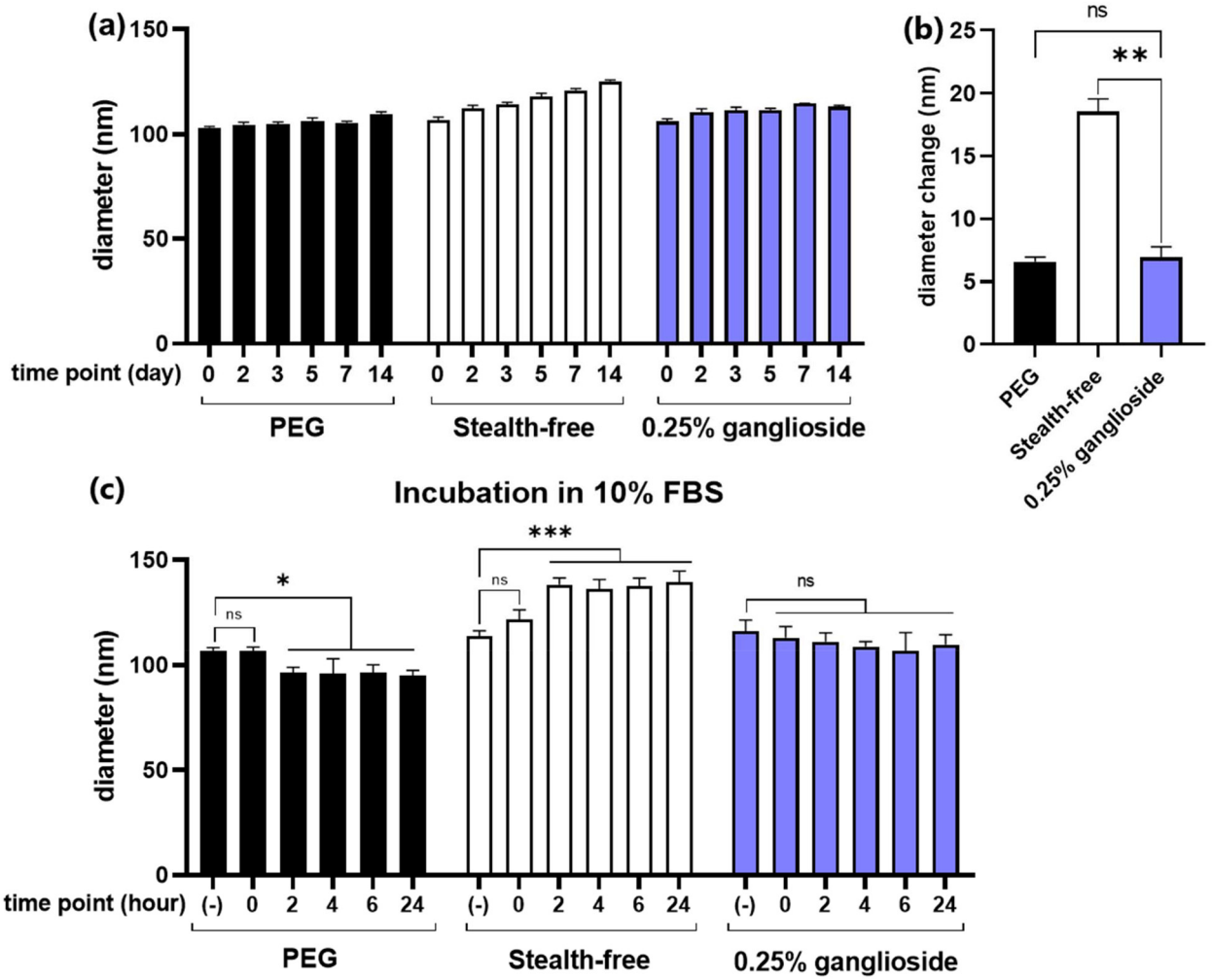

Fig. 5 Particle characterization upon cold storage and serum incubation. (a) Size measurement of PEG-LNPs, stealth-free LNPs, and optimized ganglioside-LNPs over 14 days of storage at 4 °C (N = 3). (b) Diameter change of particles after 14 days. Significance was determined using multiple t-test. (c) Size measurement of PEG-LNPs, stealth-free LNPs, and optimized ganglioside-LNPs upon particle incubation in 10% fetal bovine serum (FBS) (N = 3). Significance was determined using two-way ANOVA. Notes: (–): in the absence of serum; ns: nonsignificant; *: $p \leq 0.05$; ***: $p \leq 0.0001$.

LNPs, inhibiting effective delivery of mRNA to target tissues. Meanwhile, the incubation of ganglioside-LNPs in serum did not significantly alter the diameter, demonstrating the stealth properties conferred by ganglioside. This observation is in line with a previous study showing lower serum protein binding on the surface of ganglioside-incorporating liposomes.[27] In conclusion, ganglioside incorporation enables the formation of a steric barrier against adjacent particles and serum proteins, thereby enhancing particle stability and prolonging *in vivo* circulation.

3.4. Evaluation of *in vivo* transfection efficiency

Since the improvement in transfection efficiency was not significantly observed in comparison with stealth-free LNPs *in vitro*, the transfection efficiency of ganglioside-LNPs was then assessed *in vivo*. LNPs loaded with fLuc mRNA were systemically administered in a C57BL/6 mouse model *via* retroorbital injection. After 24 h, bioluminescence from the whole body and harvested organs (lungs, heart, spleen, kidneys, and liver) was imaged within 10–25 minutes following substrate administration. Systemic administration of ganglioside-LNPs exhibited enhanced transfection efficiencies in comparison with that of stealth-free LNPs, with a 3.3-fold increase observed in the whole body and with 3.2-fold and 3.5-fold increases in the harvested liver and spleen, respectively (Fig. 6a–d, and ESI Fig. 4†). This finding is in line with the particle characterization data obtained upon incubation in serum, in which ganglioside incorporation was demonstrated to inhibit serum protein adsorption, preventing the rapid clearance of particles (Fig. 5c). Although the transfection efficiency of ganglioside-LNPs in the liver was lower than that of PEG-LNPs (ESI Fig. 5†), these results demonstrate the potential of ganglioside-LNPs as an *in vivo* PEG-free mRNA delivery platform. Additionally, the improvement conferred by ganglioside could

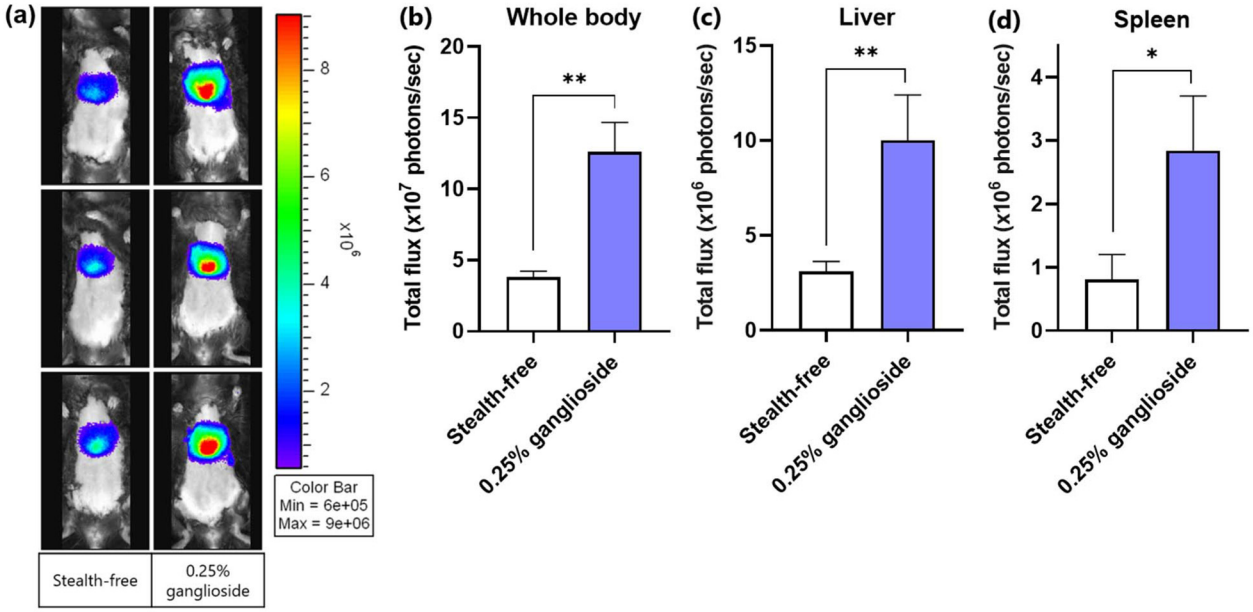

Fig. 6 Evaluation of the *in vivo* transfection efficiencies of optimized ganglioside-LNPs. (a) Whole body bioluminescence images of C57BL/6 mice 24 h after retroorbital injection of LNPs. (b) Quantification of the bioluminescence signal observed in the whole body in (a), (c and d) Quantification of the bioluminescence signal observed in *ex vivo* liver (c) and spleen (d) (N = 3). Bioluminescence data were quantified as total flux (photons per s). Stealth-free LNPs were treated as a control. Significance was determined using unpaired t-test. Note: *: $p \leq 0.05$; **: $p \leq 0.01$.

be attributed to its terminal units: sialic acid and galactose. Sialic acid is a ligand of CD169, a marker of macrophages in the marginal zone of the spleen.[38] The incorporation of sialic acid-containing glycolipids into liposomes was found to mediate specific uptake by CD169-expressing macrophages.[39] Galactose is a ligand of the asialoglycoprotein receptor (ASGPR), which is primarily expressed on hepatocytes.[40] The galactosylation of nanoparticles was observed to augment gene delivery into hepatocytes mediated by the ASGPR.[41] Therefore, the sialic acid and galactose units of ganglioside could be responsible for the increased transfection in the spleen and liver through receptor-mediated endocytosis, respectively.

Previous studies have utilized PEG substitutes with properties similar to ganglioside, such as hydrophilic and anionic.[42–44] Hydrophilic surfaces attract and retain a layer of water molecules, forming a physical barrier that prevents proteins from coming into direct contact with the nanoparticle surface.[45] Additionally, anions can create repulsive electrostatic forces against the similarly charged regions of proteins, reducing the likelihood of protein adsorption.[45] Reduced protein adsorption helps maintain the physicochemical stability of nanoparticles, ensuring that they retain their intended size and charge, thereby improving their therapeutic potential.[46] This study suggests that the hydrophilic and anionic properties of ganglioside play an important role in conferring stealth properties to LNPs by reducing serum protein adsorption and improving the stability of LNPs, thereby enhancing the *in vivo* transfection efficiency compared to stealth-free LNPs.

This study suggests the utilization of glycolipids to stabilize LNPs for the effective delivery of mRNA. Other glycolipids, *e.g.* galactolipids, cerebrosides, and globosides, could be explored in future works to discover other potential endogenous molecules that can confer stealth properties on LNPs. With a view to further improve the functionality of ganglioside-LNPs, glycoengineering of ganglioside could be conducted in the future. Engineering of the carbohydrate chains can modify the properties of ganglioside, including its pharmacokinetics and pharmacodynamics.[47] One potential approach could be to modify the length of the hydrophilic chain of ganglioside in order to control the steric barrier on the nanoparticles. Another approach is to glycoengineer the terminal residue of ganglioside with a targeting ligand in order to mediate organ- or cell type-specific tropism.

4. Conclusion

Nanoparticle stability is one of the most important aspects in developing an effective mRNA delivery platform. Instead of synthetic polyethylene glycol, glycolipids, as natural molecules in our cell membrane, can be utilized to impart stealth properties to nanoparticles. Several reports demonstrated an enhanced pharmacokinetic profile of liposomes incorporating ganglioside, which is attributed to the presence of a hydrophilic moiety akin to the PEG chain. Therefore, ganglioside has been considered as a potential substitute for PEG in conferring stealth characteristics to LNPs. *In vitro* screening resulted in an optimized ganglioside-LNP composition of 50%, 10%, 39.25%, and 0.25% of MC3, helper lipid DSPC, cholesterol, and ganglioside, respectively, and an N/P ratio of 3 : 1.

This formulation satisfied all criteria of physicochemical characteristics and elicited a 1.3-fold improvement in transfection efficiency in HEK293T cells compared to PEG-LNPs. In addition, the optimized composition conferred stealth properties, preventing particle aggregation, as demonstrated by particle characterization upon cold storage. Moreover, the evaluation of particle diameter following incubation in serum indicated that ganglioside incorporation inhibited serum protein adsorption, suggesting reduced susceptibility to particle clearance during systemic circulation. This finding is consistent with the *in vivo* assessment, where ganglioside-LNP treatment exhibited 3.3-, 3.2-, and 3.5-fold enhancements of transfection efficiencies in the whole body, liver, and spleen, respectively, compared to stealth-free LNPs. In conclusion, this study showcases the use of ganglioside for providing stealth properties to LNPs, reducing particle aggregation and interaction with serum proteins, thereby facilitating the *in vivo* delivery of mRNA. This study also highlights the potential of glycolipids as endogenous molecules offering an alternative to synthetic PEG-lipids to confer stability to nanoparticles.

Author contributions

Y. S. P. and J.-H. P. conceived and designed the research. Y. S. P., M. J., K. Y., E. F., Y. J. K. and J. H. C. carried out the experiments. Y. S. P., M. J., K. Y., and E. F. analyzed the data. Y. S. P. and J.-H. P. wrote the manuscript.

Data availability

The data used in this study are available from the corresponding author on reasonable request.

Conflicts of interest

The authors declare no competing interests.

Acknowledgements

This work was supported by the Basic Science Research Program of the National Research Foundation funded by the Ministry of Science and Information and Communication Technologies (ICT), Republic of Korea (NRF-2021R1A2C2094074), and De Novo Biotherapeutics.

References

1 X. Hou, T. Zaks, R. Langer and Y. Dong, Lipid Nanoparticles for mRNA Delivery, *Nat. Rev. Mater.*, 2021, **6**(12), 1078–1094, DOI: **10.1038/s41578-021-00358-0**.

2 K. A. Hajj and K. A. Whitehead, Tools for Translation: Non-Viral Materials for Therapeutic mRNA Delivery, *Nat. Rev. Mater.*, 2017, **2**(10), 17056, DOI: **10.1038/natrevmats.2017.56**.

3 J. Kim, Y. Eygeris, M. Gupta and G. Sahay, Self-Assembled mRNA Vaccines, *Adv. Drug Delivery Rev.*, 2021, **170**, 83–112, DOI: **10.1016/j.addr.2020.12.014**.

4 D. Pei and M. Buyanova, Overcoming Endosomal Entrapment in Drug Delivery, *Bioconjugate Chem.*, 2019, **30**(2), 273–283, DOI: **10.1021/acs.bioconjchem.8b00778**.

5 P. C. Trivedi, J. J. Bartlett and T. Pulinilkunnil, Lysosomal Biology and Function: Modern View of Cellular Debris Bin, *Cells*, 2020, **9**(5), 1131, DOI: **10.3390/cells9051131**.

6 V. Gote, P. K. Bolla, N. Kommineni, A. Butreddy, P. K. Nukala, S. S. Palakurthi and W. Khan, A Comprehensive Review of mRNA Vaccines, *Int. J. Mol. Sci.*, 2023, **24**(3), 2700, DOI: **10.3390/ijms24032700**.

7 J. A. Kulkarni, P. R. Cullis and R. van der Meel, Lipid Nanoparticles Enabling Gene Therapies: From Concepts to Clinical Utility, *Nucleic Acid Ther.*, 2018, **28**(3), 146–157, DOI: **10.1089/nat.2018.0721**.

8 M. Schlich, R. Palomba, G. Costabile, S. Mizrahy, M. Pannuzzo, D. Peer and P. Decuzzi, Cytosolic Delivery of Nucleic Acids: The Case of Ionizable Lipid Nanoparticles, *Bioeng. Transl. Med.*, 2021, **6**(2), e10213, DOI: **10.1002/btm2.10213**.

9 L. R. Baden, H. M. El Sahly, B. Essink, K. Kotloff, S. Frey, R. Novak, D. Diemert, S. A. Spector, N. Rouphael, C. B. Creech, J. McGettigan, S. Khetan, N. Segall, J. Solis, A. Brosz, C. Fierro, H. Schwartz, K. Neuzil, L. Corey, P. Gilbert, H. Janes, D. Follmann, M. Marovich, J. Mascola, L. Polakowski, J. Ledgerwood, B. S. Graham, H. Bennett, R. Pajon, C. Knightly, B. Leav, W. Deng, H. Zhou, S. Han, M. Ivarsson, J. Miller and T. Zaks, Efficacy and Safety of the mRNA-1273 SARS-CoV-2 Vaccine, *N. Engl. J. Med.*, 2021, **384**(5), 403–416, DOI: **10.1056/NEJMoa2035389**.

10 F. P. Polack, S. J. Thomas, N. Kitchin, J. Absalon, A. Gurtman, S. Lockhart, J. L. Perez, G. Pérez Marc, E. D. Moreira, C. Zerbini, R. Bailey, K. A. Swanson, S. Roychoudhury, K. Koury, P. Li, W. V. Kalina, D. Cooper, R. W. Frenck, L. L. Hammitt, Ö. Türeci, H. Nell, A. Schaefer, S. Ünal, D. B. Tresnan, S. Mather, P. R. Dormitzer, U. Şahin, K. U. Jansen and W. C. Gruber, Safety and Efficacy of the BNT162b2 mRNA Covid-19 Vaccine, *N. Engl. J. Med.*, 2020, **383**(27), 2603–2615, DOI: **10.1056/NEJMoa2034577**.

11 T. Pilishvili, Interim Estimates of Vaccine Effectiveness of Pfizer-BioNTech and Moderna COVID-19 Vaccines Among Health Care Personnel—33 U.S. Sites, January–March 2021, *Morb. Mortal. Wkly. Rep.*, 2021, **70**, 753–758.

12 S. Dong, J. Wang, Z. Guo, Y. Zhang, W. Zha, Y. Wang, C. Liu, H. Xing and X. Li, Efficient Delivery of VEGFA mRNA for Promoting Wound Healing via Ionizable Lipid Nanoparticles, *Bioorg. Med. Chem.*, 2023, **78**, 117135, DOI: **10.1016/j.bmc.2022.117135**.

13 I. Lai, S. Swaminathan, V. Baylot, A. Mosley, R. Dhanasekaran, M. Gabay and D. W. Felsher, Lipid Nanoparticles That Deliver IL-12 Messenger RNA Suppress

Tumorigenesis in MYC Oncogene-Driven Hepatocellular Carcinoma, *J. Immunother. Cancer*, 2018, **6**(1), 125, DOI: 10.1186/s40425-018-0431-x.

14 C. Huang, X. Duan, J. Wang, Q. Tian, Y. Ren, K. Chen, Z. Zhang, Y. Li, Y. Feng, K. Zhong, Y. Wang, L. Zhou, G. Guo, X. Song and A. Tong, Lipid Nanoparticle Delivery System for mRNA Encoding B7H3-Redirected Bispecific Antibody Displays Potent Antitumor Effects on Malignant Tumors, *Adv. Sci.*, 2023, **10**(3), 2205532, DOI: 10.1002/advs.202205532.

15 M. Qiu, Z. Glass, J. Chen, M. Haas, X. Jin, X. Zhao, X. Rui, Z. Ye, Y. Li, F. Zhang and Q. Xu, Lipid Nanoparticle-Mediated Codelivery of Cas9 mRNA and Single-Guide RNA Achieves Liver-Specific in Vivo Genome Editing of Angptl3, *Proc. Natl. Acad. Sci. U. S. A.*, 2021, **118**(10), e2020401118, DOI: 10.1073/pnas.2020401118.

16 E. Kenjo, H. Hozumi, Y. Makita, K. A. Iwabuchi, N. Fujimoto, S. Matsumoto, M. Kimura, Y. Amano, M. Ifuku, Y. Naoe, N. Inukai and A. Hotta, Low Immunogenicity of LNP Allows Repeated Administrations of CRISPR-Cas9 mRNA into Skeletal Muscle in Mice, *Nat. Commun.*, 2021, **12**(1), 7101, DOI: 10.1038/s41467-021-26714-w.

17 A. Sarode, Y. Fan, A. E. Byrnes, M. Hammel, G. L. Hura, Y. Fu, P. Kou, C. Hu, F. I. Hinz, J. Roberts, S. G. Koenig, K. Nagapudi, C. C. Hoogenraad, T. Chen, D. Leung and C.-W. Yen, Predictive High-Throughput Screening of PEGylated Lipids in Oligonucleotide-Loaded Lipid Nanoparticles for Neuronal Gene Silencing, *Nanoscale Adv.*, 2022, **4**(9), 2107–2123, DOI: 10.1039/D1NA00712B.

18 J. Conniot, J. M. Silva, J. G. Fernandes, L. C. Silva, R. Gaspar, S. Brocchini, H. F. Florindo and T. S. Barata, Cancer Immunotherapy: Nanodelivery Approaches for Immune Cell Targeting and Tracking, *Front. Chem.*, 2014, **2**, 105.

19 J. S. Suk, Q. Xu, N. Kim, J. Hanes and L. M. Ensign, PEGylation as a Strategy for Improving Nanoparticle-Based Drug and Gene Delivery, *Adv. Drug Delivery Rev.*, 2016, **99**(Pt A), 28–51, DOI: 10.1016/j.addr.2015.09.012.

20 O. M. Feeney, H. D. Williams, C. W. Pouton and C. J. H. Porter, 'Stealth' Lipid-Based Formulations: Poly (Ethylene Glycol)-Mediated Digestion Inhibition Improves Oral Bioavailability of a Model Poorly Water Soluble Drug, *J. Controlled Release*, 2014, **192**, 219–227, DOI: 10.1016/j.jconrel.2014.07.037.

21 T. Kolter, Ganglioside Biochemistry, *ISRN Biochem.*, 2012, **2012**, 506160, DOI: 10.5402/2012/506160.

22 S. Sipione, J. Monyror, D. Galleguillos, N. Steinberg and V. Kadam, Gangliosides in the Brain: Physiology, Pathophysiology and Therapeutic Applications, *Front. Neurosci.*, 2020, **14**, 572965, DOI: 10.3389/fnins.2020.572965.

23 R. K. Yu, Y.-T. Tsai, T. Ariga and M. Yanagisawa, Structures, Biosynthesis, and Functions of Gangliosides—An Overview, *J. Oleo Sci.*, 2011, **60**(10), 537–544.

24 C.-G. Gölander, J. N. Gölander, K. Lim, P. Claesson, P. Stenius and J. D. Andrade, Properties of Immobilized PEG Films and the Interaction with Proteins, in *Poly (Ethylene Glycol) Chemistry: Biotechnical and Biomedical Applications*, ed. J. M. Harris, Springer US, Boston, MA, 1992, pp. 221–245, Topics in Applied Chemistry, DOI: 10.1007/978-1-4899-0703-5_15.

25 D. Liu and L. Huang, pH-Sensitive, Plasma-Stable Liposomes with Relatively Prolonged Residence in Circulation, *Biochim. Biophys. Acta, Biomembr.*, 1990, **1022**(3), 348–354, DOI: 10.1016/0005-2736(90)90284-U.

26 K. Maruyama, A. Okamoto, O. Ishida, S. Kojima, A. Suginaka, L. Huang and M. Iwatsuru, Biodistribution and Antitumor Effect of Adriamycin Encapsulated in Long-Circulating Liposomes Containing Amphipathic Polyethylene Glycol or Ganglioside GM1, *J. Liposome Res.*, 1994, **4**(1), 701–723, DOI: 10.3109/08982109409037067.

27 A. Chonn and P. R. Cullis, Ganglioside GM1 and Hydrophilic Polymers Increase Liposome Circulation Times by Inhibiting the Association of Blood Proteins, *J. Liposome Res.*, 1992, **2**(3), 397–410, DOI: 10.3109/08982109209010217.

28 M. Jayaraman, S. M. Ansell, B. L. Mui, Y. K. Tam, J. Chen, X. Du, D. Butler, L. Eltepu, S. Matsuda, J. K. Narayanannair, K. G. Rajeev, I. M. Hafez, A. Akinc, M. A. Maier, M. A. Tracy, P. R. Cullis, T. D. Madden, M. Manoharan and M. J. Hope, Maximizing the Potency of siRNA Lipid Nanoparticles for Hepatic Gene Silencing In Vivo**, *Angew. Chem., Int. Ed.*, 2012, **51**(34), 8529–8533, DOI: 10.1002/anie.201203263.

29 K. Okuda, Y. Sato, K. Iwakawa, K. Sasaki, N. Okabe, M. Maeki, M. Tokeshi and H. Harashima, On the Size-Regulation of RNA-Loaded Lipid Nanoparticles Synthesized by Microfluidic Device, *J. Controlled Release*, 2022, **348**, 648–659, DOI: 10.1016/j.jconrel.2022.06.017.

30 K. Paunovska, A. J. Da Silva Sanchez, C. D. Sago, Z. Gan, M. P. Lokugamage, F. Z. Islam, S. Kalathoor, B. R. Krupczak and J. E. Dahlman, Nanoparticles Containing Oxidized Cholesterol Deliver mRNA to the Liver Microenvironment at Clinically Relevant Doses, *Adv. Mater.*, 2019, **31**(14), 1807748, DOI: 10.1002/adma.201807748.

31 P. C. Soema, G.-J. Willems, W. Jiskoot, J.-P. Amorij and G. F. Kersten, Predicting the Influence of Liposomal Lipid Composition on Liposome Size, Zeta Potential and Liposome-Induced Dendritic Cell Maturation Using a Design of Experiments Approach, *Eur. J. Pharm. Biopharm.*, 2015, **94**, 427–435, DOI: 10.1016/j.ejpb.2015.06.026.

32 C. Cayabyab, A. Brown, G. Tharmarajah and A. Thomas, *mRNA Lipid Nanoparticles: Robust Low-Volume Production for Screening High-Value Nanoparticle Materials*, Precis. Nanosyst. Inc, 2018, pp. 1–7.

33 S. S. Nogueira, A. Schlegel, K. Maxeiner, B. Weber, M. Barz, M. A. Schroer, C. E. Blanchet, D. I. Svergun, S. Ramishetti, D. Peer, P. Langguth, U. Sahin and H. Haas, Polysarcosine-Functionalized Lipid Nanoparticles for Therapeutic mRNA Delivery, *ACS Appl. Nano Mater.*, 2020, **3**(11), 10634–10645, DOI: 10.1021/acsanm.0c01834.

34 Y. Gao, K. Yang, A. N. Shelling and Z. Wu, Nanotechnology-Enabled COVID-19 mRNA Vaccines, *Encyclopedia*, 2021, **1**(3), 773–780, DOI: **10.3390/encyclopedia1030059**.

35 M. E. Ritchie, Reaction and Diffusion Thermodynamics Explain Optimal Temperatures of Biochemical Reactions, *Sci. Rep.*, 2018, **8**(1), 11105, DOI: **10.1038/s41598-018-28833-9**.

36 S. C. Wilson, J. L. Baryza, A. J. Reynolds, K. Bowman, M. E. Keegan, S. M. Standley, N. P. Gardner, P. Parmar, V. O. Agir, S. Yadav, A. Zunic, C. Vargeese, C. C. Lee and S. Rajan, Real Time Measurement of PEG Shedding from Lipid Nanoparticles in Serum via NMR Spectroscopy, *Mol. Pharm.*, 2015, **12**(2), 386–392, DOI: **10.1021/mp500400k**.

37 B. Romberg, W. E. Hennink and G. Storm, Sheddable Coatings for Long-Circulating Nanoparticles, *Pharm. Res.*, 2008, **25**(1), 55–71, DOI: **10.1007/s11095-007-9348-7**.

38 A. Gallud, M. J. Munson, K. Liu, A. Idström, H. M. G. Barriga, S. R. Tabaei, N. Aliakbarinodehi, M. Ojansivu, Q. Lubart, J. J. Doutch, M. N. Holme, L. Evenäs, L. Lindfors, M. M. Stevens, A. Collén, A. Sabirsh, F. Höök and E. K. Esbjörner, Time Evolution of PEG-Shedding and Serum Protein Coronation Determines the Cell Uptake Kinetics and Delivery of Lipid Nanoparticle Formulated mRNA, *bioRxiv*, 2021,preprint, p 2021.08.20.457104. DOI: **10.1101/2021.08.20.457104**.

39 J. Grabowska, M. A. Lopez-Venegas, A. J. Affandi and J. M. M. den Haan, CD169+ Macrophages Capture and Dendritic Cells Instruct: The Interplay of the Gatekeeper and the General of the Immune System, *Front. Immunol.*, 2018, **9**, 2472, DOI: **10.3389/fimmu.2018.02472**.

40 M. K. Nijen Twilhaar, L. Czentner, J. Grabowska, A. J. Affandi, C. Y. J. Lau, K. Olesek, H. Kalay, C. F. van Nostrum, Y. van Kooyk, G. Storm and J. M. M. den Haan, Optimization of Liposomes for Antigen Targeting to Splenic CD169+ Macrophages, *Pharmaceutics*, 2020, **12**(12), 1138, DOI: **10.3390/pharmaceutics12121138**.

41 D. Roggenbuck, M. G. Mytilinaiou, S. V. Lapin, D. Reinhold and K. Conrad, Asialoglycoprotein Receptor (ASGPR): A Peculiar Target of Liver-Specific Autoimmunity, *Autoimmun. Highlights*, 2012, **3**(3), 119–125, DOI: **10.1007/s13317-012-0041-4**.

42 B. Thapa, P. Kumar, H. Zeng and R. Narain, Asialoglycoprotein Receptor-Mediated Gene Delivery to Hepatocytes Using Galactosylated Polymers, *Biomacromolecules*, 2015, **16**(9), 3008–3020, DOI: **10.1021/acs.biomac.5b00906**.

43 V. Andretto, M. Repellin, M. Pujol, E. Almouazen, J. Sidi-Boumedine, T. Granjon, H. Zhang, K. Remaut, L. P. Jordheim, S. Briançon, I. S. Keil, F. Vascotto, K. C. Walzer, U. Sahin, H. Haas, D. Kryza and G. Lollo, Hybrid Core-Shell Particles for mRNA Systemic Delivery, *J. Controlled Release*, 2023, **353**, 1037–1049, DOI: **10.1016/j.jconrel.2022.11.042**.

44 S. de M. Barros, L. A. Avila, S. K. Whitaker, K. E. Wilkinson, P. Sukthankar, E. I. C. Beltrão and J. M. Tomich, Branched Amphipathic Peptide Capsules: Different Ratios of the Two Constituent Peptides Direct Distinct Bilayer Structures, Sizes, and DNA Transfection Efficiency, *Langmuir*, 2017, **33**(28), 7096–7104, DOI: **10.1021/acs.langmuir.7b00912**.

45 N. Kunte, M. Westerfield, E. McGraw, J. Choi, T. Akinsipe, S. K. Whitaker, A. Brannen, P. Panizzi, J. M. Tomich and L. A. Avila, Evaluation of Transfection Efficacy, Biodistribution, and Toxicity of Branched Amphiphilic Peptide Capsules (BAPCs) Associated with mRNA, *Biomater. Sci.*, 2022, **10**(24), 6980–6991, DOI: **10.1039/D2BM01314B**.

46 S. Salmaso and P. Caliceti, Stealth Properties to Improve Therapeutic Efficacy of Drug Nanocarriers, *J. Drug Delivery*, 2013, 2013, e374252, DOI: **10.1155/2013/374252**.

47 T. U. Wani, S. N. Raza and N. A. Khan, Nanoparticle Opsonization: Forces Involved and Protection by Long Chain Polymers, *Polym. Bull.*, 2020, **77**(7), 3865–3889, DOI: **10.1007/s00289-019-02924-7**.